Antiviral Research 83 (2009) 35–44

Contents lists available at ScienceDirect

Antiviral Research

journal homepage: www.elsevier.com/locate/antiviral

Mechanism of the antiviral effect of hydroxytyrosol on influenza virus appears to involve morphological change of the virus

Kentaro Yamada[a,1], Haruko Ogawa[a,*], Ayako Hara[a], Yukio Yoshida[a], Yutaka Yonezawa[a], Kazuji Karibe[a], Vuong Bui Nghia[a], Hiroyuki Yoshimura[b], Yu Yamamoto[c], Manabu Yamada[c], Kuniyasu Nakamura[c], Kunitoshi Imai[a]

[a] Research Center for Animal Hygiene and Food Safety, Obihiro University of Agriculture and Veterinary Medicine, Obihiro, Hokkaido 080-8555, Japan
[b] Eisai Food & Chemical Co., Ltd., Nihonbashi, Tokyo 103-0027, Japan
[c] Research Team of Viral Diseases, National Institute of Animal Health, Tsukuba, Ibaraki 305-0856, Japan

ARTICLE INFO

Article history:
Received 29 September 2008
Received in revised form 28 February 2009
Accepted 11 March 2009

Keywords:
Hydroxytyrosol
Influenza A virus
Antiviral effect
Envelope
Morphology

ABSTRACT

Hydroxytyrosol (HT), a small-molecule phenolic compound, inactivated influenza A viruses including H1N1, H3N2, H5N1, and H9N2 subtypes. HT also inactivated Newcastle disease virus but not bovine rotavirus, and fowl adenovirus, suggesting that the mechanism of the antiviral effect of HT might require the presence of a viral envelope. Pretreatment of MDCK cells with HT did not affect the propagation of H9N2 virus subsequently inoculated onto the cells, implying that HT targets the virus but not the host cell. H9N2 virus inactivated with HT retained unaltered hemagglutinating activity and bound to MDCK cells in a manner similar to untreated virus. Neuraminidase activity in the HT-treated virus also remained unchanged. However, in the cells inoculated with HT-inactivated H9N2 virus, neither viral mRNA nor viral protein was detected. Electron microscopic analysis revealed morphological abnormalities in the HT-treated H9N2 virus. Most structures found in the HT-treated virus were atypical of influenza virions, and localization of hemagglutinin was not necessarily confined on the virion surface. These observations suggest that the structure of H9N2 virus could be disrupted by HT.

1. Introduction

Hydroxytyrosol (HT) is a small-molecule phenolic compound found in the leaves and fruits of olive (*Olea eurolaea*) as a metabolite of oleuropein (Ole), which is one of the major polyphenolic components of olive products (Fig. 1). HT can be purified from olive products (Ciafardini et al., 1994; Lee-Huang et al., 2007a; Visioli et al., 1998a), and can also be prepared by chemical synthesis (Capasso et al., 1999; Espín et al., 2001; Lee-Huang et al., 2007a; Tuck et al., 2000). The polyphenolic compounds contained in olive leaf extracts and olive oils have been reported to exert various bioactivities, including antioxidant (Coni et al., 2000; Visioli et al., 1995, 1998a,b, 2001), anti-inflammatory (Beauchamp et al., 2005; Bitler et al., 2005; Pacheco et al., 2007), and antimicrobial activities against bacteria, fungi, and mycoplasma (Aziz et al., 1998; Bisignano et al., 1999; Furneri et al., 2002). Among them, the beneficial effects of olive phenols on coronary heart diseases have been extensively studied (Covas, 2007).

It has also been reported that olive leaf extracts exhibit antiviral activities against human immunodeficiency virus type 1 (HIV-1) (Bao et al., 2007; Lee-Huang et al., 2003, 2007a,b) and viral haemorrhagic septicaemia rhabdovirus (Micol et al., 2005). Lee-Huang et al. (2003) have demonstrated the strong activity of olive leaf extract against HIV-1, in which the compound mixture inhibited acute infection and cell-to-cell transmission of HIV-1, and ultimately suppressed viral replication in the infected cells. Their recent studies identified Ole and HT as the HIV-1 inhibitors contained in the olive leaf extracts. In these studies, Ole and HT inhibited not only the fusion between viral and cellular membranes but also the integrase activity of the virus. A molecular modeling study revealed that Ole and HT bound to the conserved hydrophobic pocket on the surface of the HIV-1 envelope protein gp41, which is a transmembrane subunit of HIV-1 envelope glycoprotein. The results of a computational study suggested that HT is the predicted main moiety for the binding to gp41. Binding of HT to gp41 appears to cause a conformational change in the glycoprotein, which could result in the inhibition of viral entry into the target cells (Bao et al., 2007; Lee-Huang et al., 2007a,b). These studies suggest that Ole and HT might be useful against other viruses with type I transmembrane envelope glycoproteins.

Ma et al. (2001) have previously reported that Ole isolated from the fruits of *Ligustrum lucidum* exhibits significant antiviral activ-

* Corresponding author. Tel.: +81 155 495893; fax: +81 155 495893.
E-mail address: hogawa@obihiro.ac.jp (H. Ogawa).
[1] Present address: Central Research Laboratories, Nippon Zenyaku Kogyo Co., Ltd., Koriyama, Fukushima 963-0196, Japan.

0166-3542/$ – see front matter © 2009 Elsevier B.V. All rights reserved.
doi:10.1016/j.antiviral.2009.03.002

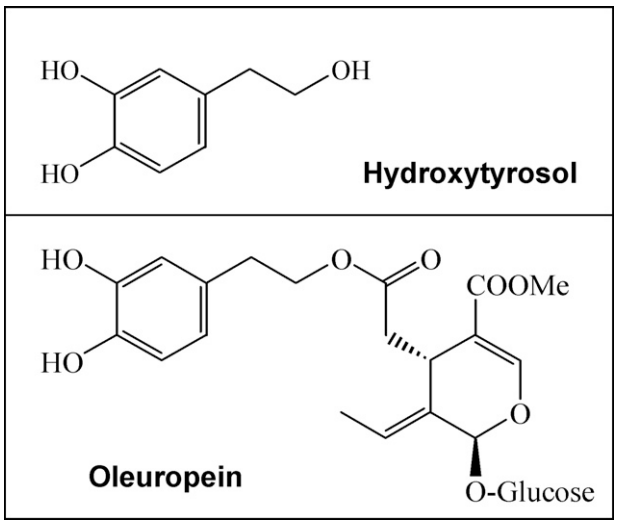

Fig. 1. Chemical structure of hydroxytyrosol and oleuropein.

ities against respiratory syncytial virus and parainfluenza type 3 virus, but not against herpes simplex type 1 virus and influenza A virus, although all these viruses possess type I transmembrane envelope glycoproteins. These results might suggest that the antiviral effect of Ole and HT is applicable to a limited number of viruses that have the relevant binding sites for these compounds.

In the present study, the antiviral effect of HT was investigated using influenza A viruses, Newcastle disease virus (NDV), group A bovine rotavirus (BRV), and fowl adenovirus (FAV). Among the viruses tested, HT was effective against the enveloped viruses, but not against the non-enveloped viruses. We attempted to elucidate the mechanism of the antiviral effect of HT against influenza virus, and found morphological abnormalities in the HT-treated influenza virus.

2. Experimental/materials and methods

2.1. Cells and viruses

Avian influenza viruses A/chicken/Yokohama/aq55/01 (H9N2) (Eto and Mase, 2003) and A/chicken/Yamaguchi/7/04 (H5N1), and NDV Ibaraki/85 strain were provided by the National Institute of Animal Health, Japan. Human influenza viruses A/Hokkaido/30/2000 (H1N1) and A/Hokkaido/52/98 (H3N2) were from the Hokkaido Institute of Public Health, Japan. BRV Lincoln strain was from the Hokkaido Livestock Research Institute, Japan, and serotype 1 FAV 99ZH strain from the Zennoh Institute of Animal Health, Japan.

The H9N2 virus was propagated in the allantoic cavity of 10-day-old embryonated chicken eggs, and purified by ultracentrifugation using 30% and 60% sucrose solutions. The protein content of the purified virus was measured by using a Micro BCA protein assay kit (Pierce, Rockford, IL). H5N1 virus and NDV were also propagated in embryonated chicken eggs, and the obtained allantoic fluid was used as virus stock solution. Human influenza viruses were grown in MDCK cells, and the culture supernatant served as the virus stock solution. The infectivity of influenza viruses was tested in MDCK cells. Upon the inoculation of influenza viruses other than the H5N1 virus, the medium was replaced with virus growth medium (VGM), which was prepared according to the WHO Manual on Animal Influenza Diagnosis and Surveillance (WHO Manual). The infectivities of NDV, BRV, and FAV were tested in MDBK, MA104, and LMH, respectively. Dulbecco's modified Eagle's medium (Nissui Pharmaceutical Co., Ltd., Tokyo, Japan) was used for culturing the MDCK, MDBK, and MA104 cells. LMH cells were cultured in Waymouth's medium (Invitrogen, Carlsbad, CA). Each cell medium was supplemented with 10% fetal bovine serum and 2 mM L-glutamine. Prior to the inoculation of MA104 cells with BRV, the virus was pretreated with 10 μg/ml trypsin at 37 °C for 30 min, then the trypsinized virus was added to the cells in which the medium had been replaced with VGM.

2.2. Treatment of viruses and cells with HT

HT (98.3% purity), purified from olive leaf extracts, was provided by Eisai Food & Chemical Co., Ltd. (Tokyo, Japan). HT was dissolved in phosphate-buffered saline (PBS) and diluted to concentrations ranging from 0.1 to 1000 μg/ml (0.65–6535.9 μM). The viruses ($10^{5.2}$–$10^{6.6}$ $TCID_{50}$/ml) were added to HT solutions of different concentration and maintained at room temperature for a predetermined period of time. Following the treatment, the virus titer in the mixture was measured by inoculating serial 10-fold dilutions (beginning with a 1:10 dilution) of the mixture into the host cells. The $TCID_{50}$ was calculated by the Behrens-Karber method based on the cytopathic effect (CPE) observed on day 5 post-inoculation (p.i.). The effect of benzalkonium chloride (BC) on the H9N2 virus was also tested as a control compound with virucidal activity. The BC solutions at the concentrations between 0.002% and 0.016% were prepared using commercially available 10% BC solution (Osvan, Nihon Pharmaceutical Co., Ltd., Tokyo, Japan).

In order to test the effect of HT on the cells, the cells were first cultured with a medium containing HT for 24 h. The cell medium was then replaced with fresh medium lacking HT, the cells having been initially washed with PBS. The serially diluted HT-untreated virus was inoculated into the cells, and the virus titers measured in the HT-treated and untreated cells were compared.

The cytotoxicity of HT on the cells was analyzed by measuring the lactate dehydrogenase released from the cells using a Cytotoxicity Detection kit (Roche, Mannheim, Germany). The percentage cytotoxicity was calculated by the following equation using the obtained absorbance values, from which the absorbance values in the corresponding background control were subtracted: [(Experimental release − spontaneous release)/(maximum release − spontaneous release)] × 100%.

The hemagglutination titer of the H9N2 virus was measured in 96-well microplates with V-shaped bottom. The virus was serially diluted in a twofold dilution with PBS. Into each well containing 50 μl of the virus solution, an equal volume of 0.8% chicken erythrocytes suspended in PBS was added. Following mechanical vibration, the plates containing the mixture of virus and erythrocytes were kept at room temperature, and the results were recorded after 30 min. The titer was expressed as the reciprocal of the highest dilution of the virus showing complete hemagglutination. The assay was triplicated for each virus dilution, and the HA titer determined represents the titer identically recorded with all of the three or two out of the three tests. We considered the difference greater than 2 times to be a significant difference in hemagglutination titer.

The neuraminidase (NA) activity of the virus was measured according to the WHO Manual. Briefly, the virus was serially diluted in a twofold dilution with PBS and incubated with Fetuin (Sigma, St. Louis, MO) at 37 °C for 18 h. The amount of sialic acid liberated was determined chemically with the thiobarbituric acid that develops color in proportion to the concentration of free sialic acid. The color developed was measured at a wavelength of 549 nm.

2.3. Real-time reverse transcription-polymerase chain reaction (RRT-PCR)

Total RNA was extracted from the MDCK cells inoculated with either the HT-treated or untreated H9N2 virus using Isogen (Nippon Gene, Tokyo, Japan). The RNA thus obtained was

transcribed into cDNA by SuperScript III Reverse Transcriptase (Invitrogen) under the following conditions: 50 °C for 60 min and 70 °C for 10 min. Real-time reverse transcription-polymerase chain reaction (RRT-PCR) was performed in order to detect the viral RNA (vRNA) and viral mRNA (vmRNA) by using the LightCycler-FastStart DNA Master SYBR Green I kit (Roche). In order to detect vRNA, the extracted RNA was reverse transcribed using the Uni12 primer 5′-AGCAAAAGCAGG-3′. For vmRNA detection, the oligo-dT primer was used in the RT reaction. Partial segments of the H9N2 virus genes were amplified using the following primer sets (respective product sizes are in parentheses): PB2, 5′-CTGGGAGCAGATGTACACTC-3′ and 5′-ACAGCTTGTTCCTCAGTTGG-3′ (207 bp); PB1, 5′-GTGTCAGATGGAGGGCCAAA-3′ and 5′-TCGCAACGGCATCATACTCC-3′ (214 bp); PA, 5′-AAGGCTCCATCGGAAAGGTG-3′ and 5′-AGCCCTCCAAGATCGAAGGT-3′ (169 bp); HA, 5′-AGTGCATGGAGACAATTCGG-3′ and 5′-CATTGGACATGGCCCAGAAC-3′ (200 bp); NP, 5′-GCAACTGCTGGTCTTACCCA-3′ and 5′-CCGAATCAGCTCCATCACCA-3′ (201 bp); NA, 5′-GCATAGCATGGTCCAGCTCA-3′ and 5′-CCTGATGCACTTCCATCCGT-3′ (220 bp); M_1, 5′-GACGTTCCATGGAGCAAAGG-3′ and 5′-GCCTGATTAGTGGGTTGGTG-3′ (204 bp); NS_2, 5′-TAGTGGGCGAAATCTCACCA-3′ and 5′-ATCCTCATCGCTGCTTCTCC-3′ (161 bp). The thermal profile included the following cycles: denaturation at 95 °C for 10 min followed by 45 cycles at 95 °C for 10 s, 55 or 56 °C for 5 s, and 72 °C for 6–9 s. RRT-PCR for detecting the housekeeping gene *GAPDH* was also performed using the following primer set: 5′-GGGGCCATCCACAGTCTTCT-3′ and 5′-GCCAAAAGGGTCATCATCTC-3′. Following the amplification, a melting curve analysis was performed to confirm the specificity of the reaction. The product size was confirmed by 1% agarose gel electrophoresis. The threshold cycle (C_T) value for each sample was calculated by determining the point at which the fluorescence exceeded the threshold limit.

2.4. Flow cytometry analysis

The virus bound to the cell surface was analyzed by flow cytometry. MDCK cells were inoculated with the HT-treated or untreated H9N2 virus at a concentration of 10 μg/ml and incubated at 4 °C for 1 h. The cells were then stained with the monoclonal antibody (mAb) against hemagglutinin (HA) labeled with Alexa Fluor 488 by using a Zenon Mouse IgG Labeling kit (Invitrogen) according to the Manufacturer's instructions. Stained cells were fixed with 1% paraformaldehyde solution.

The presence of H9N2 virus within the cells was also analyzed by flow cytometry using a mAb against the viral nucleoprotein (NP). MDCK cells were inoculated with either the HT-treated or untreated virus at a concentration of 1 μg/ml and incubated at 37 °C for 3 or 24 h. The cells were then harvested, followed by fixation and permealization using a BD Cytofix/Cytoperm kit (BD Biosciences, San Jose, CA). Subsequently, the cells were intracellulary stained with anti-NP mAb, which was labeled with Alexa Fluor 488.

Stained cells were analyzed using a FACSCanto flow cytometer (BD Biosciences). The mAbs used for cell staining were produced in our laboratory as previously described (J. Virol. Methods, submitted for publication).

2.5. Electron microscopic analysis

The HT-treated or untreated H9N2 virus was attached to a carbon-coated collodion grid (Nisshin EM Co. Ltd., Tokyo, Japan), and negatively stained with 2% phosphotungstic acid, pH 6.8 (PTA). In order to detect the HA protein using a specific antibody, the virus on the grid was first blocked with 1% bovine serum albumin in PBS for 30 min, stained with anti-HA mAb biotinylated using Biotin-OSu (Dojindo, Kumamoto, Japan) for 30 min, and then incubated with streptavidin immunogold conjugate (BBInternational, Cardiff, UK) for 60 min. The virus was stained with the PTA, and examined using a Hitachi H7500 electron microscope (Tokyo, Japan).

3. Results

3.1. Antiviral effect of HT on enveloped and non-enveloped viruses

The antiviral effect of HT on the H9N2 virus, NDV, BRV, and FAV was investigated by measuring the virus titers 24 h after mixing

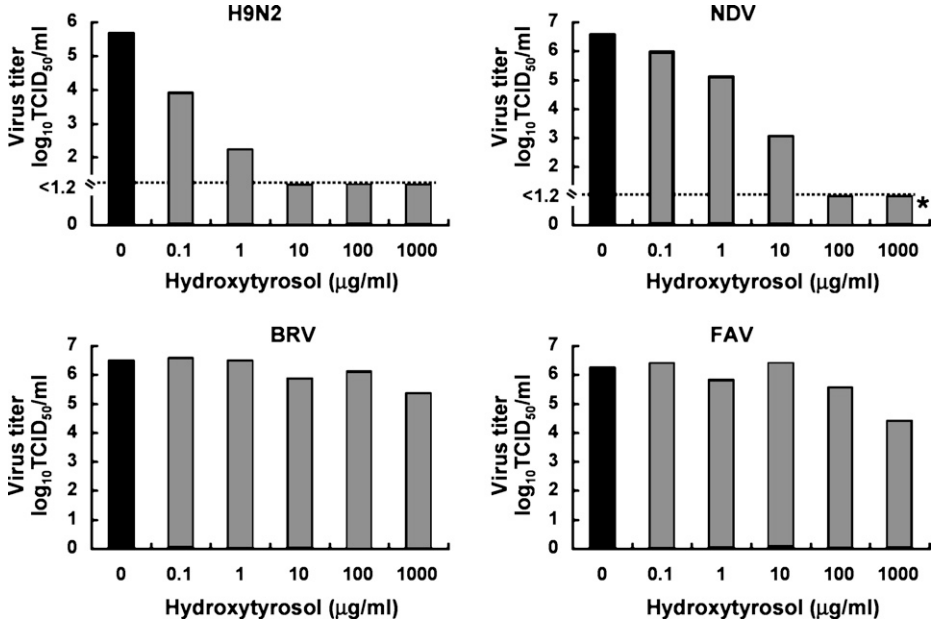

Fig. 2. Comparison of the antiviral effects of HT on a variety of viruses. The viruses were treated with the HT solution at room temperature for 24 h. The treated virus was serially diluted in a 10-fold dilution beginning with a 1:10 dilution, and inoculated into the cells to evaluate the virus titer. The cells for titration of each virus are described in Section 2. Asterisks represent the results obtained at a HT concentration slightly cytotoxic to the cells. Black bars represent the titer of the control virus that had been kept at room temperature for 24 h in the absence of HT.

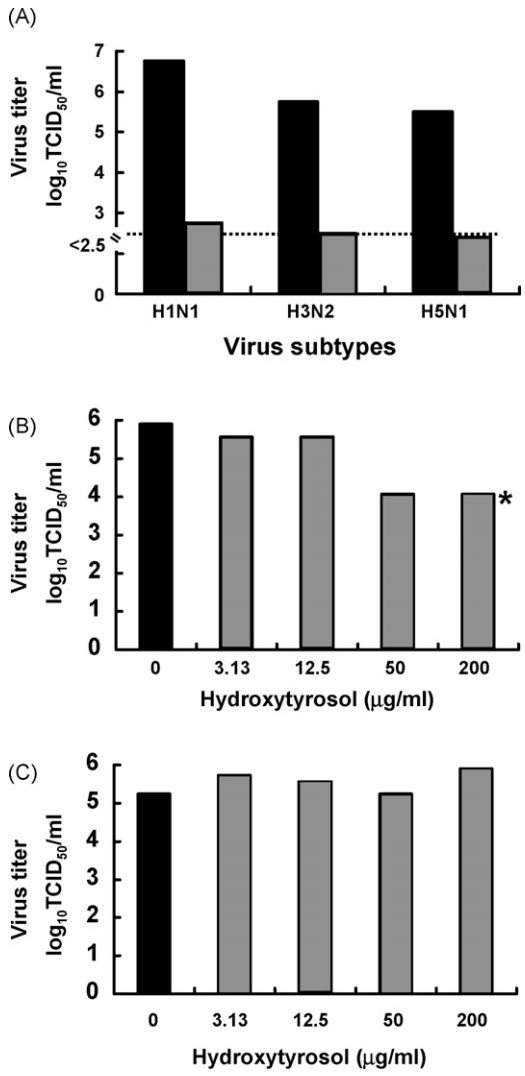

Fig. 3. Antiviral effect of HT on influenza viruses. (A) Effect of HT on H1N1, H3N2 and H5N1 viruses. The viruses were treated with HT (1000 μg/ml) at room temperature for 24 h. The treated virus was serially diluted in a 10-fold dilution beginning with a 1:10 dilution, and inoculated into MDCK cells to evaluate the virus titer. Black bars represent the titer of the control virus that had been kept at room temperature for 24 h in the absence of HT. (B) Propagation of H9N2 virus inoculated into MDCK cells concurrently with the addition of HT to the cell. The virus was inoculated into MDCK cells immediately after mixing with HT solution. Final concentrations of HT in the cell medium are shown. Asterisk represents the results obtained at the HT concentration slightly cytotoxic to the cells. (C) Propagation of H9N2 virus in MDCK cells pretreated with HT. The cells had been cultured in the presence of HT for 24 h. Then the cell medium was replaced with the one lacking HT, and inoculated with untreated H9N2 virus.

the virus with different concentrations of HT. HT concentration-dependently lowered the titer of the two enveloped viruses at concentrations between 0.1 and 10 μg/ml (0.65–65 μM) for the H9N2 virus and 0.1 and 100 μg/ml (0.65–650 μM) for NDV (Fig. 2). HT also lowered the titers of other influenza viruses including H1N1, H3N2, and H5N1 subtypes (Fig. 3A). In contrast, the virus titers of the non-enveloped BRV and FAV were virtually unchanged by treatment with the HT solution, although the virus titers of BRV and FAV appeared to be slightly decreased at the concentration of 1000 μg/ml HT (Fig. 2). The 1:10 dilution of the inoculum containing 1000 μg/ml HT yielded the highest concentration of HT (100 μg/ml) within the cells. The concentration of 100 μg/ml HT was the threshold dose that did not cause a cytotoxic effect against MDCK, LMH, and MA104 cells, but was slightly cytotoxic (7.2% cytotoxicity) to MDBK cells (data not shown).

3.2. Kinetics of the antiviral effect of HT on the H9N2 virus

In HT solutions with concentrations greater than 12.5 μg/ml, the titer of the H9N2 virus was lowered by >1.5 log in 1 h, and further decreased in a time-dependent manner (Fig. 4). The virus titer decreased by >4 log and reached undetectable levels at 12 h following the inoculation of the virus into 200 μg/ml HT. At 12.5 and 50 μg/ml HT, the virus titer decreased by >4 log at 24 h. In contrast, the titer of the H9N2 virus declined in BC solutions at a much faster speed. The titer decreased nearly 4 log in 0.016% and 0.008% BC solutions within 10 min and 3 h, respectively (Fig. 5).

If the H9N2 virus was inoculated into MDCK cells concurrently with the addition of HT to the cells, the virus titer decreased by >1.5 log at a concentration higher than 50 μg/ml HT, but only a minor change was observed at lower concentrations of HT (Fig. 3B). Since the HT concentrations indicated in Fig. 3B present the final concentrations of HT contained in the cell medium, the final concentrations of HT are 10 times higher than those in Figs. 2 and 4. The results presented in Fig. 3B indicate that if HT gets into contact with the H9N2 virus in the presence of cells it is unable to significantly alter the virus titer, even at the semi-cytotoxic dose.

The H9N2 virus was able to propagate in the cells that had been cultured in a medium containing HT for 24 h as in the untreated cells. Thus, pretreatment of the cells with HT did not affect the titer of the H9N2 virus subsequently inoculated onto the cells (Fig. 3C).

3.3. HA activity and NA activity of the HT-treated H9N2 virus

HA and NA activities were compared between the HT-treated and untreated H9N2 virus. The HT-treated virus retained an hemagglutination titer at an equivalent level to the untreated virus (Table 1). NA activity also did not differ between the HT-treated and untreated virus (Fig. 6). In flow cytometric analysis, HA was detected on the surface of cells inoculated with the HT-treated virus at a level similar to the cells inoculated with untreated virus (Fig. 7).

3.4. Suppression of viral RNA synthesis in the cells inoculated with the HT-treated H9N2 virus

The synthesis of vmRNA and vRNA in MDCK cells inoculated with the HT-treated or untreated H9N2 virus was analyzed at 0.2, 1, 3, 6, and 24 h after the inoculation of the virus. A portion of 8 segments of the influenza virus RNA was amplified by RRT-PCR. In the cells inoculated with untreated H9N2 virus, the C_T values for each of the segments of vmRNA continued to decline between 1 and 6 or 24 h p.i. (Fig. 8). The C_T values for vRNA in the untreated virus-inoculated cells underwent a similar transition (data not shown). These results indicated active replication of the virus in the cells following the viral inoculation. On the other hand, in the cells inoculated with the HT-treated H9N2 virus, neither the C_T values for vmRNA (Fig. 8) nor those for vRNA (data not shown) changed notably until 24 h p.i.

Table 1
Hemagglutination titer of H9N2 virus treated with HT.

Treatment with HT (μg/ml)	Hemagglutination titer/treatment time				
	1 h	3 h	6 h	12 h	24 h
200	64	64	64	64	64
50	64	64	64	64	64
12.5	64	32	64	64	64
3.13	64	64	64	64	64
0	64	64	64	64	32

The H9N2 virus was treated with the HT solution as in Fig. 1, and hemagglutination titers were measured using chicken erythrocytes.

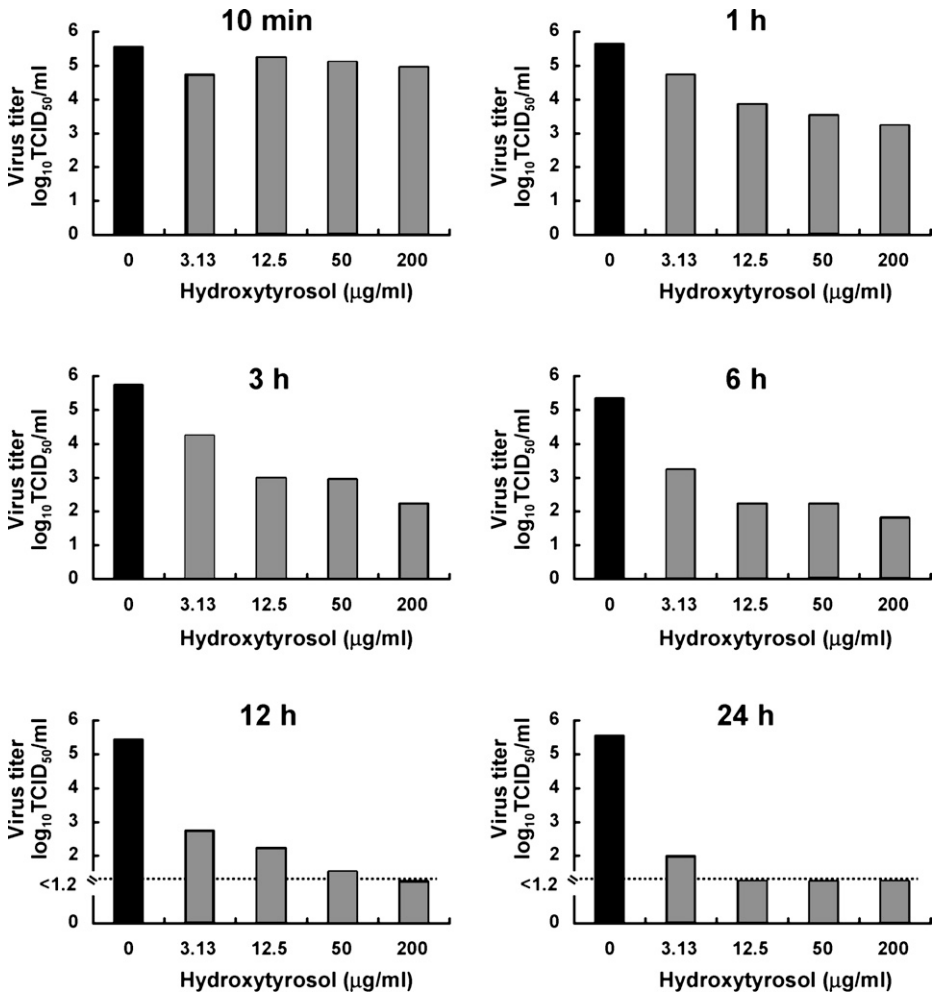

Fig. 4. Antiviral effect of HT on H9N2 virus at various concentrations and different treatment times. The H9N2 virus was treated with the HT solution at room temperature for the defined period of time. The treated virus was serially diluted in a 10-fold dilution beginning with a 1:10 dilution, and inoculated into MDCK cells. Black bars represent the titer of the control virus that had been kept at room temperature for the corresponding period of time in the absence of HT.

3.5. Lack of viral protein synthesis in the cells inoculated with the HT-treated H9N2 virus

In order to detect viral protein synthesis in the cells following the inoculation of the H9N2 virus, viral NP was intracellularly stained with anti-NP mAb. In the cells inoculated with untreated H9N2 virus, NP was detected at 3 h p.i., but only at a low level. However, the amount of NP increased dramatically at 24 h p.i., indicating the vigorous synthesis of viral protein. In contrast, NP protein was undetectable in the cells inoculated with the HT-treated H9N2 virus at 24 h p.i., suggesting a lack of viral protein synthesis (Fig. 9).

3.6. Morphological abnormality in the HT-treated virus

In the electron microscopic analysis of negatively stained virus, the virion shapes of the untreated H9N2 virus were found to be typical of influenza virus. These included spherical, elliptical, and filamentous virions. Each particle was surrounded by a layer, from the surface of which projected numerous spikes; these spikes are assumed to be HA and NA spikes (Fig. 10A). Binding of colloidal gold confirmed that HA proteins are localized on the spikes (Fig. 11A). In contrast, few particles were detected in the HT-treated H9N2 virus as typical influenza virions, and many ambiguous structures were found instead. These structures appeared to lack the layer of spikes on the surface. Some virion-shaped particles with spiked surfaces were observed; however, the outline of these particles was not as distinct as the untreated virus (Fig. 10B). Localization of HA was not necessarily confined to the virion surface, rather it was found to be diffuse (Fig. 11B).

4. Discussion

The present study demonstrated the antiviral effect of HT on influenza virus and NDV. HT effectively lowered the virus titer of the two enveloped viruses in a dose-dependent manner. In contrast, the virus titer of all the non-enveloped viruses tested, which included BRV and FAV, was not affected by HT (Figs. 2 and 3). These results suggest that the viral envelope is likely to be involved in the mechanism of the HT antiviral effect.

Our observations appear to be similar to those of previous studies on the antiviral effect of HT on HIV-1, in which HT and Ole (a precursor substance of HT) dose-dependently inhibited HIV-1 infection and replication. It has been reported that HT and Ole bind to the HIV–gp41 fusion domain, thereby interfering with the formation of the gp41 fusion-active core and resulting in the inhibition of fusion, based on the results obtained by molecular modeling studies (Bao et al., 2007; Lee-Huang et al., 2003, 2007a, b). HT (mol wt: 153) is a main metabolite of Ole (mol wt: 539). It is interesting to note that such a small molecule can effectively block the protein–protein interaction in the HIV–gp41 fusion domain, crucially disturbing viral cell entry. If the influenza virus protein has a binding site for HT in the domain essential for cell entry, HT might

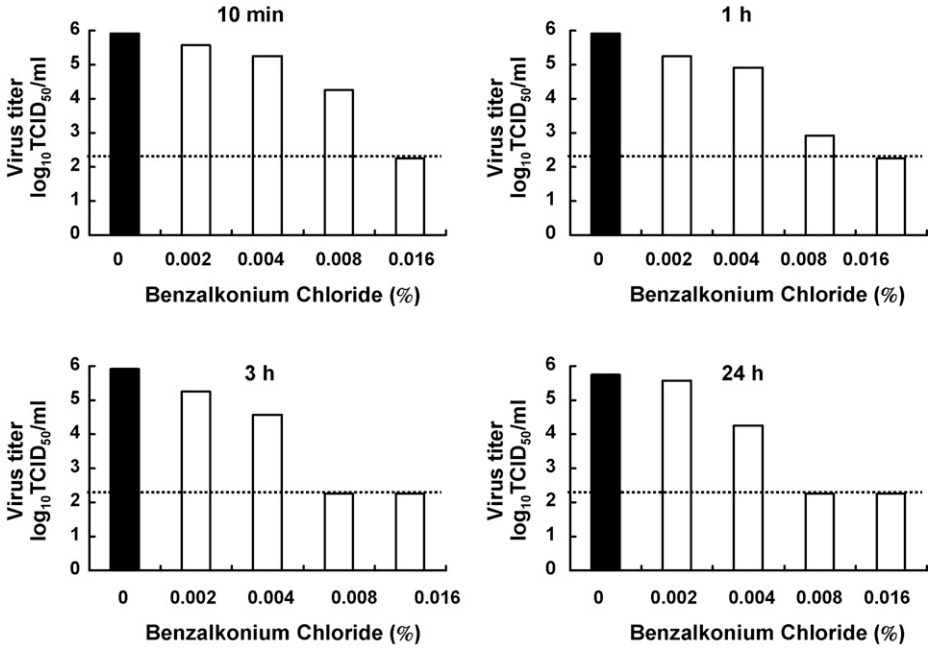

Fig. 5. Antiviral effect of BC on H9N2 virus at various concentrations and different treatment times. The experiment was performed as in Fig. 4. Black bars represent the titer of the control virus that had been kept at room temperature for the corresponding period of time in the absence of BC. Broken lines represent the level of virus titer detectable in the assay. Because the addition of the solution containing BC was toxic to MDCK cells even at the concentration of 0.0008% (10 times dilution of the virus solution treated with 0.008% BC solution), the virus titer detectable in the assay was higher than with HT.

act on influenza virus. In the present study, the HT-treated H9N2 virus retained unchanged HA activity and bound to MDCK cells in a manner similar to untreated virus (Table 1 and Fig. 7); however, viral replication was suppressed in these cells (Figs. 8 and 9). It should be explored whether the HT-treated H9N2 virus was internalized into the cells following its binding to the cell. In addition, investigations should be undertaken in order to determine whether the binding of HT to the viral proteins occurs at the sites involved in the fusion process. We are currently trying to determine if the envelope of influenza virus has a binding site for HT like HIV-1 gp41 does, and, further, if the HT binding indeed affects the viral cell entry.

On the other hand, the antiviral mechanism of HT on the H9N2 virus and HIV-1 should not necessarily be the same, since the cell entry mechanism of these viruses is not identical. In fact, the kinetics of the antiviral effects of HT on the H9N2 virus seemed to be different to those on HIV-1. It was reported that HT and Ole inhibited the syncytial formation in cell-to-cell transmission of HIV-1 and the synthesis of the viral core protein p24 in the assay co-culturing HIV-infected H9 cells and uninfected MT-2 target cells (Lee-Huang et al., 2007a). These results suggest that the antiviral activity of HT on HIV-1 is effective under circumstances in which the target cells have already been infected with the virus. In the present study, the antiviral effect of HT on the H9N2 virus was found to be a time-dependent but relatively slow process. HT required a period between 1 and 3 h to lower the H9N2 virus titer by >1.5 log, and between 12 and 24 h to decrease the titer by >4 log in MDCK cells (Fig. 4). The addition of HT to the cells simultaneously with the viral inoculation caused only a marginal antiviral effect (Fig. 3B). Thus, it is necessary for HT to treat H9N2 virus, unlike HIV-1, in the absence of target cells for a certain period of time in order to facilitate its inactivation. Interestingly, we found that Ole does not exert any antiviral effect to the H9N2 virus (data not shown). This further suggests that the mechanism of antiviral effect of HT against influenza virus would be different from that against HIV-1. The results obtained in this study also suggest the following: (1) the antiviral effect of HT on the H9N2 virus is attributable to the direct effect of HT on the virus and not via an indirect effect on the cells (Fig. 2C); (2) HT appears to interfere with the early stage of viral infection rather than the later stage when proliferated virus are released from the cells. Indeed, the NA activity of the H9N2 virus was not affected by HT (Fig. 6).

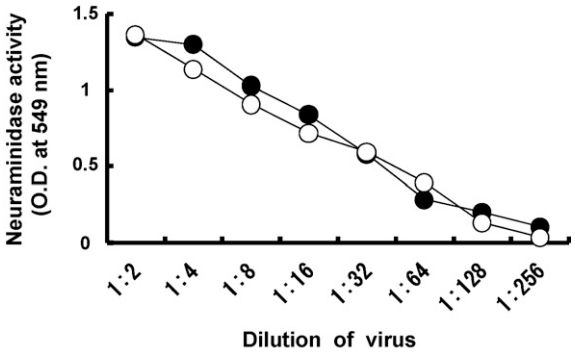

Fig. 6. NA activity of HT-treated H9N2 virus. Following a 24-h treatment of the H9N2 virus with 200 μg/ml HT, the virus solutions were serially diluted to 1:2, and the NA activity of the solutions was measured. The data shown are representative of two separate experiments with similar results. NA activities of untreated virus (○) and virus treated with HT (●).

It has been reported that CYSTUS052, a polyphenol rich plant extract from a special variety of *Cistus incanus*, exerts a potent anti-influenza virus activity (Ehrhardt et al., 2007). In these studies, treatment of the cells with CYSTUS052 resulted in a reduction of progeny virus titers up to two logs if cells were either pre-incubated with CYSTUS052 or the extract was added simultaneously with the virus. The titer reduction was also observed if the virus was preincubated with CYSTUS052. The results suggested that CYSTUS052 appears to inhibit the viral entry process, and indeed CYSTUS052 was found to interfere the binding of the viral HA to cellular receptors. Although the active moiety of CYSTUS052 has not been known, the antiviral mechanism of HT seems to be different from that of CYSTUS052.

Since HT requires pre-incubation time in order to be effective to influenza virus and the time needed for the viral inactivation

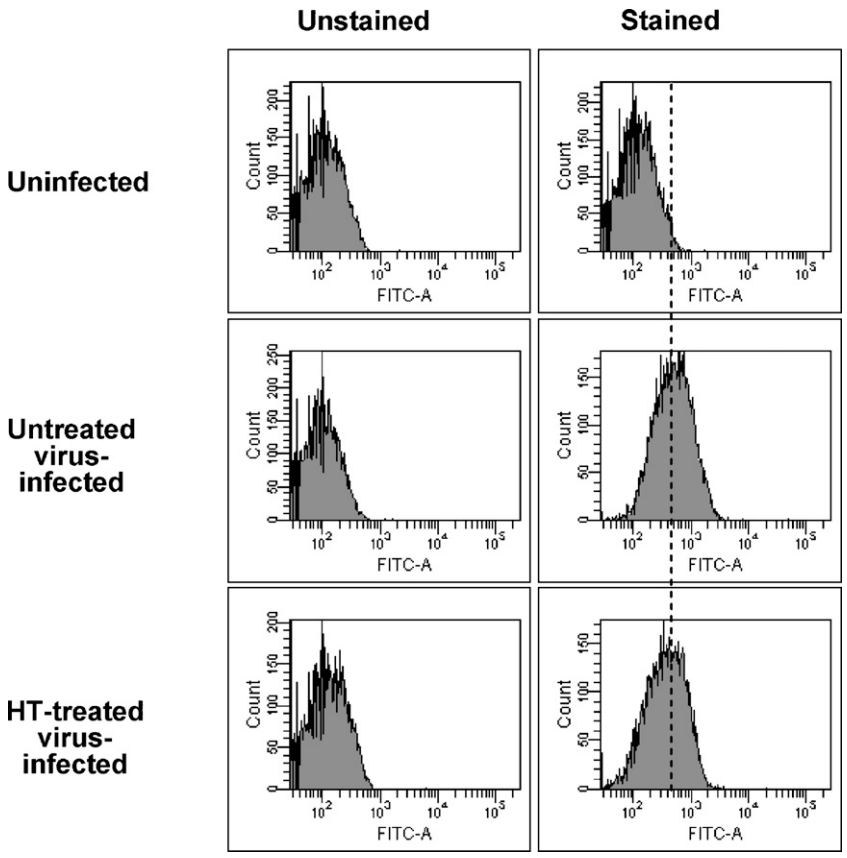

Fig. 7. Presence of viral HA protein on the surface of the cells inoculated with HT-treated H9N2 virus. The surface of MDCK cells was stained with anti-HA mAb labeled with Alexa Fluor 488 1 h after the inoculation of untreated virus or the virus treated with 200 μg/ml HT for 24 h.

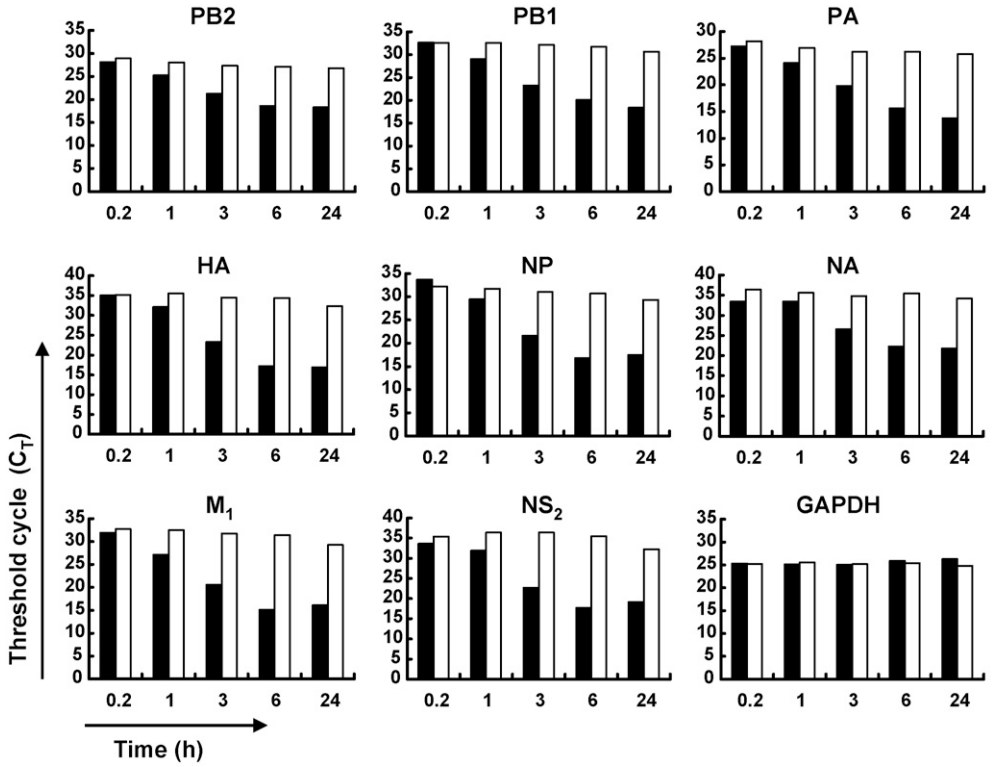

Fig. 8. Suppression of vmRNA synthesis in the cells inoculated with HT-treated H9N2 virus. The vmRNAs for each of 8 segments of the virus were amplified by RRT-PCR using total RNA extracted from the MDCK cells at 0.2, 1, 3, 6, and 24 h after the inoculation of either HT-treated or untreated H9N2 virus and oligo-dT primer. Representative data from two separate experiments are shown in the Figure. Cycle numbers for threshold (C_T) in the RRT-PCR are presented. The black and white bars represent results obtained with untreated virus and the virus treated with 200 μg/ml HT for 24 h, respectively.

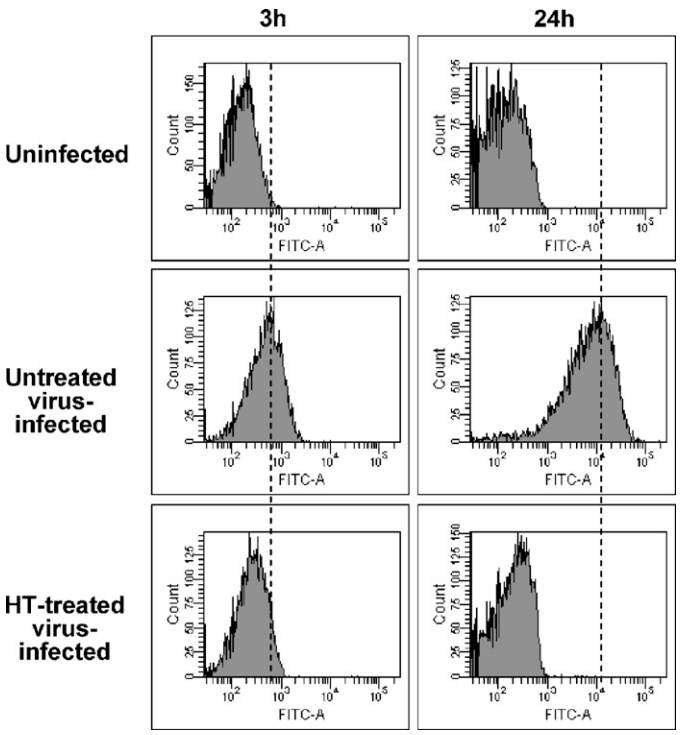

Fig. 9. Lack of viral NP protein in the cells inoculated with HT-treated H9N2 virus. MDCK cells were harvested 3 or 24 h after the inoculation of untreated virus or the virus treated with 200 μg/ml HT for 24 h. The cells were permeabilized and stained with anti-NP mAb labeled with Alexa Fluor 488.

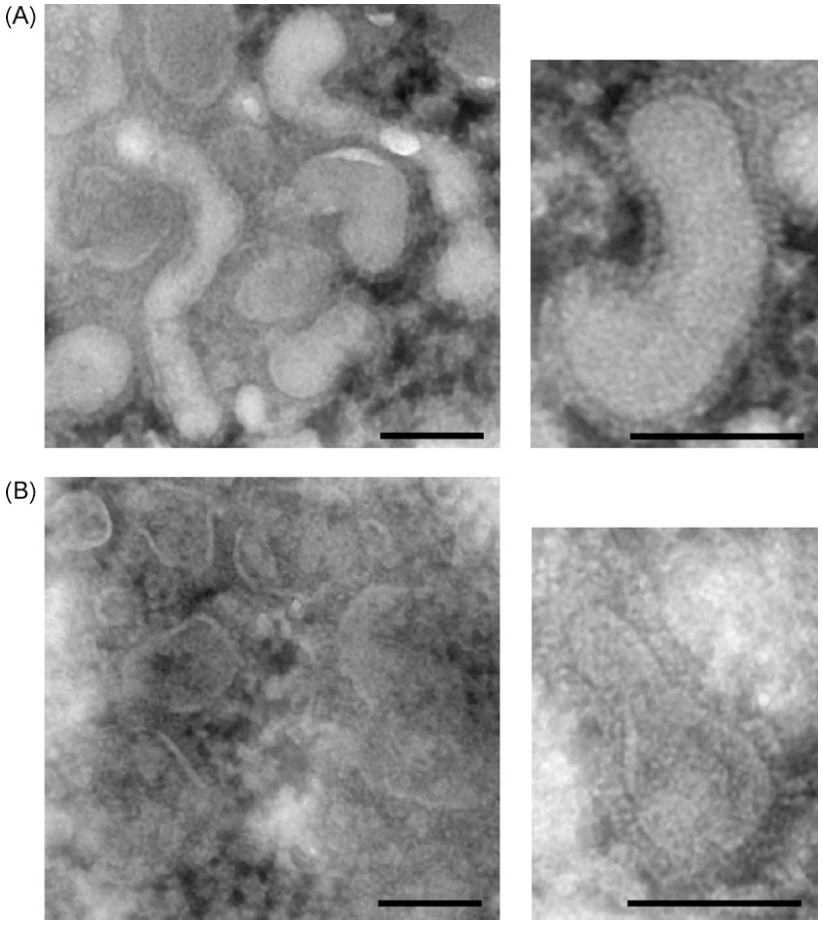

Fig. 10. Electron microscopic analysis of HT-treated H9N2 virus. The negatively stained virus was analyzed. The bar represents 100 nm. (A) Untreated virus; (B) the virus treated with 200 μg/ml of HT for 24 h.

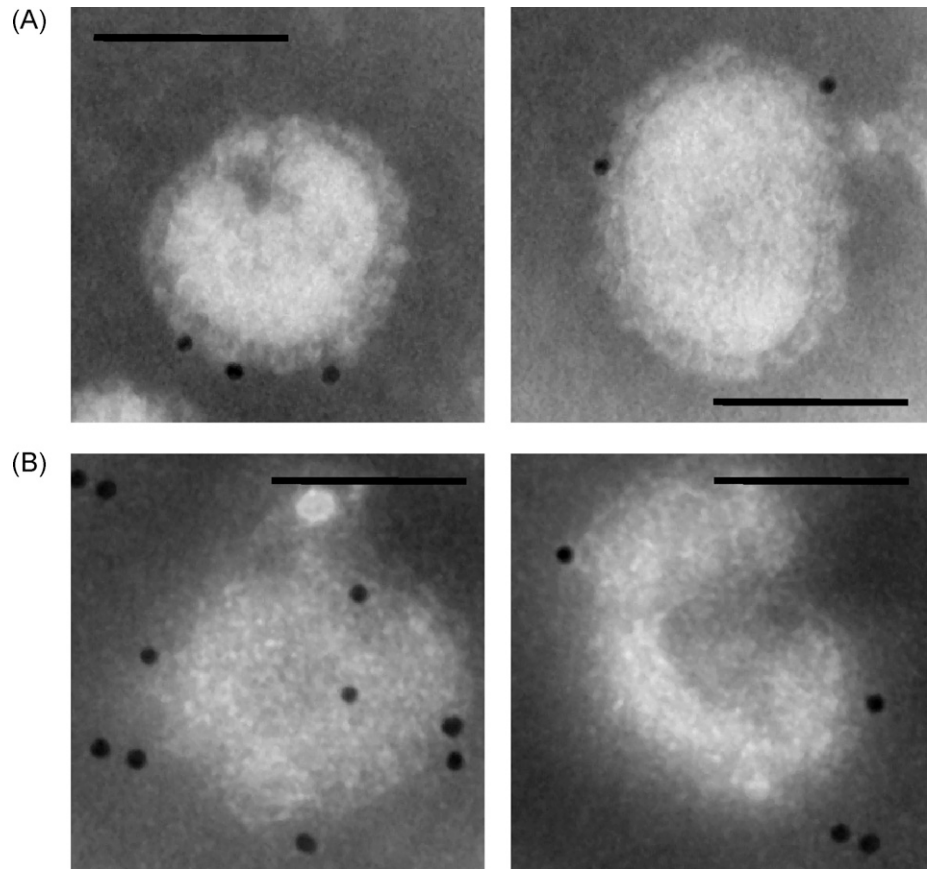

Fig. 11. Immunoelectron microscopic analysis of HT-treated H9N2 virus. The virus was stained with biotinylated anti-HA mAb followed by streptavidin immunogold conjugate. The bar represents 100 nm. (A) Untreated virus; (B) the virus treated with 200 μg/ml of HT for 24 h.

seems to be longer than those of the currently available disinfectants such as BC (Figs. 4 and 5), it will not be applicable for clinical use as it is. Bioavailability of HT has been studied because of increased interests to its antioxidant effect. It was reported that HT underwent extensive metabolism and urinary excretion *in vivo*. The highest concentration of HT in urine was observed in the first 4 h after the ingestion of olive oil in humans (Caruso et al., 2001; Miró-Casas et al., 2001). Such a high rate metabolism should also hamper the clinical usage of HT. However, clarifying the antiviral mechanism of HT might open the way to utilize this chemical available from natural products in influenza control. Alternatively, the information obtained in the study may enable HT to become a platform for developing novel antiviral agents.

The HT-treated H9N2 virus was morphologically analyzed under the electron microscope. It was found that most of the structures observed in the HT-treated H9N2 virus had been ill-defined. These structures appeared to be lacking surface spikes. HA protein seemed not be confined only to the surface of virion-shaped particles. These results suggest that the structure of viral envelope could be disrupted by HT (Figs. 10 and 11). Suppression of vmRNA synthesis and lack of viral NP protein observed within the cells inoculated with HT-treated H9N2 virus (Figs. 8 and 9) might be the results of an insufficiency in viral binding, viral uncoating or other steps in viral infection. Although we could detect the unchanged HA and NA activities in the HT-treated H9N2 virus (Table 1 and Figs. 6 and 7), the results may not necessarily represent the activities of intact HA and NA that are attached to the virion surface. We are currently investigating whether the activities of HA and NA detected in the HT-treated virus are caused by the envelope-bound HA and NA or the envelope-unbound free HA and NA, and whether further the disruption of viral envelope could result in the generation of HA and NA detached from the virion surface.

This study first demonstrated the antiviral effect of HT on influenza virus. The morphological changes observed under the electron microscope might suggest that the effect of HT to influenza virus is virucidal rather than antiviral. Additional studies are clearly required in order to clarify the crucial events that occur during the interaction of HT with the influenza virus. Although the results of the current and previous studies suggest that HT seems to act on a molecule on the viral envelope, the antiviral effect of HT may not be equivalent to all enveloped viruses. Not only the extent but also the mechanism of the antiviral effect of HT would depend on how many viral sites HT interacts with and, furthermore, how important the target sites are to the virus.

Acknowledgements

We thank Sachiko Matsuda for technical assistance. This work was partially supported by grants from the Program of Founding Research Centers for Emerging and Reemerging Infectious Diseases, and by a Grant-in-Aid for Exploratory Research (19659115) from MEXT (Japan).

References

Aziz, N.H., Farag, S.E., Mousa, L.A., Abo-Zaid, M.A., 1998. Comparative antibacterial and antifungal effects of some phenolic compounds. Microbios 93, 43–54.

Bao, J., Zhang, D.W., Zhang, J.Z., Huang, P.L., Huang, P.L., Lee-Huang, S., 2007. Computational study of bindings of olive leaf extract (OLE) to HIV-1 fusion protein gp41. FEBS Lett. 581, 2737–2742.

Beauchamp, G.K., Keast, R.S., Morel, D., Lin, J., Pika, J., Han, Q., Lee, C.H., Smith, A.B., Breslin, P.A., 2005. Phytochemistry: ibuprofen-like activity in extra-virgin olive oil. Nature 437, 45–46.

Bisignano, G., Tomaino, A., Lo Cascio, R., Crisafi, G., Uccella, N., Saija, A., 1999. On the *in vitro* antimicrobial activity of oleuropein and hydroxytyrosol. J. Pharm. Pharmacol. 51, 971–974.

Bitler, C.M., Viale, T.M., Damaj, B., Crea, R., 2005. Hydrolyzed olive vegetation water in mice has anti-inflammatory activity. J. Nutr. 135, 1475–1479.

Capasso, R., Evidente, A., Avolio, S., Solla, F., 1999. A highly convenient synthesis of hydroxytyrosol and its recovery from agricultural waste waters. J. Agric. Food Chem. 47, 1745–1748.

Caruso, D., Visioli, F., Patelli, R., Galli, C., Galli, G., 2001. Urinary excretion of olive oil phenols and their metabolites in humans. Metabolism 50, 1426–1428.

Ciafardini, G., Marsilio, V., Lanza, B., Pozzi, N., 1994. Hydrolysis of oleuropein by *Lactobacillus plantarum* strains associated with olive fermentation. Appl. Environ. Microbiol. 60, 4142–4147.

Coni, E., Di Benedetto, R., Di Pasquale, M., Masella, R., Modesti, D., Mattei, R., Carlini, E.A., 2000. Protective effect of oleuropein, an olive oil biophenol, on low density lipoprotein oxidizability in rabbits. Lipids 35, 45–54.

Covas, M.I., 2007. Olive oil and the cardiovascular system. Pharmacol. Res. 55, 175–186.

Ehrhardt, C., Hrincius, E.R., Korte, V., Mazur, I., Droebner, K., Poetter, A., Dreschers, S., Schmolke, M., Planz, O., Ludwig, S., 2007. A polyphenol rich plant extract, CYSTUS052, exerts anti influenza virus activity in cell culture without toxic side effects or the tendency to induce viral resistance. Antiviral Res. 76, 38–47.

Espín, J.C., Soler-Rivas, C., Cantos, E., Tomás-Barberán, F.A., Wichers, H.J., 2001. Synthesis of the antioxidant hydroxytyrosol using tyrosinase as biocatalyst. J. Agric. Food Chem. 49, 1187–1193.

Eto, M., Mase, M., 2003. Isolation of the Newcastle disease virus and the H9N2 influenza A virus from chicken imported from China. J. Jpn. Vet. Med. Assoc. 56, 333–339.

Furneri, P.M., Marino, A., Saija, A., Uccella, N., Bisignano, G., 2002. *In vitro* antimycoplasmal activity of oleuropein. Int. J. Antimicrob. Agents 20, 293–296.

Lee-Huang, S., Zhang, L., Huang, P.L., Chang, Y.T., Huang, P.L., 2003. Anti-HIV activity of olive leaf extract (OLE) and modulation of host cell gene expression by HIV-1 infection and OLE treatment. Biochem. Biophys. Res. Commun. 307, 1029–1037.

Lee-Huang, S., Huang, P.L., Zhang, D., Lee, J.W., Bao, J., Sun, Y., Chang, Y.T., Zhang, J., Huang, P.L., 2007a. Discovery of small-molecule HIV-1 fusion and integrase inhibitors oleuropein and hydroxytyrosol: Part I. Fusion inhibition. Biochem. Biophys. Res. Commun. 354, 872–878.

Lee-Huang, S., Huang, P.L., Zhang, D., Lee, J.W., Bao, J., Sun, Y., Chang, Y.T., Zhang, J., Huang, P.L., 2007b. Discovery of small-molecule HIV-1 fusion and integrase inhibitors oleuropein and hydroxytyrosol. Part II. Integrase inhibition. Biochem. Biophys. Res. Commun. 354, 879–884.

Ma, S.C., He, Z.D., Deng, X.L., But, P.P., Ooi, V.E., Xu, H.X., Lee, S.H., Lee, S.F., 2001. *In vitro* evaluation of secoiridoid glucosides from the fruits of *Ligustrum lucidum* as antiviral agents. Chem. Pharm. Bull. 49, 1471–1473.

Micol, V., Caturla, N., Pérez-Fons, L., Más, V., Pérez, L., Estepa, A., 2005. The olive leaf extract exhibits antiviral activity against viral haemorrhagic septicaemia rhabdovirus (VHSV). Antiviral Res. 66, 129–136.

Miró-Casas, E., Farré Albaladejo, M., Covas, M.I., Rodriguez, J.O., Menoyo Colomer, E., Lamuela Raventós, R.M., de la Torre, R., 2001. Capillary gas chromatography-mass spectrometry quantitative determination of hydroxytyrosol and tyrosol in human urine after olive oil intake. Anal. Biochem. 294, 63–72.

Pacheco, Y.M., Bermúdez, B., López, S., Abia, R., Villar, J., Muriana, F.J., 2007. Minor compounds of olive oil have postprandial anti-inflammatory effects. Br. J. Nutr. 29, 1–4.

Tuck, K.L., Tan, H.W., Hayball, P.J., 2000. Synthesis of tritium-labeled hydroxytyrosol, a phenolic compound found in olive oil. J. Agric. Food Chem. 48, 4087–4090.

Visioli, F., Bellomo, G., Montedoro, G., Galli, C., 1995. Low density lipoprotein oxidation is inhibited in vitro by olive oil constituents. Atherosclerosis 117, 25–32.

Visioli, F., Bellomo, G., Galli, C., 1998a. Free radical-scavenging properties of olive oil polyphenols. Biochem. Biophys. Res. Commun. 247, 60–64.

Visioli, F., Bellosta, S., Galli, C., 1998b. Oleuropein, the bitter principle of olives, enhances nitric oxide production by mouse macrophages. Life Sci. 62, 541–546.

Visioli, F., Caruso, D., Plasmati, E., Patelli, R., Mulinacci, N., Romani, A., Galli, G., Galli, C., 2001. Hydroxytyrosol, as a component of olive mill waste water, is dose-dependently absorbed and increases the antioxidant capacity of rat plasma. Free Radic. Res. 34, 301–305.